

# Physical Significance of Negative Yule-Nielsen n-value

J A Stephen Viggiano, Chester F Carlson Center for Imaging Science, Rochester NY 14623 (USA)

## Abstract

Negative values of Yule-Nielsen's parameter  $n$  in empirical fits have occasionally arisen. This paper examines two probable causes, ink spread and non-transparency of the ink. Three new models for single-ink halftone spectra are derived and exercised. It was necessary for the two factors to combine to consistently result in negative  $n$  in empirical fits to simulated spectra.

## Introduction

While performing model-based characterization of color halftone devices, solutions with negative Yule-Nielsen  $n$  occasionally arise. The purpose of this paper is to examine two causes for this phenomenon beyond the diffusion of light within the substrate. In order to do this, three new models of halftone behavior will be derived and exercised. In this section, a few of the existing models shall be examined as an introduction.

## The Yule-Nielsen Model

In a seminal 1951 paper, Yule and Nielsen [1] describe a model which relates the reflectance of a halftone print,  $\beta_t$ , the reflectance of the solid ink,  $\beta_s$ , and the area fraction of the halftone pattern,  $f$ . If we also account for the reflectance of the unprinted substrate,  $\beta_g$  (in 1951 it was customary to null the reflectometer on the unprinted substrate so all reflectances would be relative to its reflectance), we obtain:

$$\beta_t = \left[ (1-f) \cdot \beta_g^{1/n} + f \cdot \beta_s^{1/n} \right]^n \quad (1)$$

where  $n$  is a parameter which semi-empirically accounts for the diffusion of light within the substrate. Viggiano, after demonstrating mathematically why the model performed poorly with integrated reflectances, extended this to the spectral case, and suggested replacing the  $1/n$  with  $u$ . The Yule-Nielsen-Viggiano model (also termed the VHM-1) may be written: [2, 3]

$$\beta_{t\lambda}^u = (1-f) \cdot \beta_{g\lambda}^u + f \cdot \beta_{s\lambda}^u \quad (2)$$

The inverse of Eq (2) is also of interest; it provides  $f$  as a function of  $\beta_t$  and the parameters:

$$f = \left( \beta_{g\lambda}^u - \beta_{t\lambda}^u \right) / \left( \beta_{g\lambda}^u - \beta_{s\lambda}^u \right) \quad (3)$$

When estimating  $f$  from the spectra  $\beta_{g\lambda}$ ,  $\beta_{s\lambda}$ , and  $\beta_{t\lambda}$ , the value is usually selected by minimizing weighted reflectance error,  $\Delta E_{ab}^*$ , or a similar criterion, in Eq (2), rather than through Eq (3). Eq (3) may be applied in narrow spectral bands when the its denominator is large.

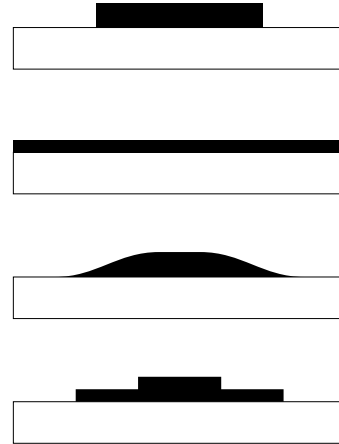


Figure 1. Profiles of dots under different degrees of volume-preserving spreading. Top: hard-edged dot; upper middle: complete ink spread; lower middle: incomplete ink spread; bottom: incomplete ink spread, approximated with core/fringe (wedding cake) model. Paper thickness is not to scale.

## Physical Significance of $n$ for $1 \leq n \leq 2$

The Yule-Nielsen model has been derived by Davies (reported by Murray) [4] for  $n = 1$ , with no diffusion of light under the dot, in which case it is referred to as the Murray-Davies model, and by Yule and Nielsen for  $n = 2$ , which corresponds to complete diffusion with transparent inks. Ruckdeschel and Hauser [5] examined incomplete diffusion (assuming transparent inks and ), and found that the parameter  $n$  was bounded between 1 and 2. Pearson [6] found that an  $n = 1.7$  minimized density error for several cases he considered, and recommended that it be used in the absence of more specific information.

## $n > 2$ in praxis

Pope [7] examined additional cases, and determined  $n$  for each by equating the  $f$  determined using microplanimetry with the  $f$  predicted using Eq (3). Many of the instances of  $n$  determined by Pope were greater than 2. The iterative search used by Pope did not converge for several cases. These were when the relative (to the substrate) density of the tint,  $D_t - D_g = \log(\beta_g) - \log(\beta_t)$ , was greater than the area fractional coverage,  $f$ , times the relative density of the solid,  $D_s - D_g = \log(\beta_g) - \log(\beta_s)$ .

## Pollack's Limit: $n \rightarrow \infty$

Pollack [8] asserted that the relative density of the tint will equal the product of the relative density of the solid and the fractional area in the limit as  $n \rightarrow \infty$ . Pollack's limit is ex-

Model	Ink Spread	Light Diffusion	Scatter in Ink?	Ink Penetration?
VHM-5	Complete	(doesn't matter)	Yes	No
VHM-6	None	Complete	Yes	No
VHM-7	Incomplete	Complete	Yes	No

**Table 1: Three models and their assumptions.**

pressed in terms of reflectances as:

$$\lim_{n \rightarrow \infty} \left[ (1-f) \cdot \beta_{g\lambda}^u + f \cdot \beta_{s\lambda}^u \right]^n = \beta_{g\lambda}^{(1-f)} \cdot \beta_{s\lambda}^f \quad (4)$$

and, in terms of absolute densities, as:

$$\lim_{n \rightarrow \infty} D_{t\lambda} = (1-f) \cdot D_{g\lambda} + f \cdot D_{s\lambda} \quad (5)$$

Eqs (4) and (5) parallel the model of Bouguer, Lambert, [9] and Beer. [10] If the ink is non-scattering and a layer of unit thickness on a substrate of reflectance  $\beta_s$  has itself reflectance  $\beta_s$ , Eq (4) will give the Bouguer-Lambert-Beer solution for a layer of thickness  $f$ . If a non-scattering ink is applied as a halftone with a fractional area  $f$  at unit thickness is smeared or spread into a continuous layer atop the substrate of thickness  $f$ , the Bouguer-Lambert-Beer law will apply, as confirmed by Arney and Yamaguchi. [11]

This is why Pollack's limit is referred to as such: it is not only a limit in the mathematical sense, but is also a limit in the physical sense. Halftone patterns printed from a non-scattering ink (which do not penetrate the substrate if it scatters optically) will have  $n \rightarrow \infty$ . The limit of halftone image production under the conditions mentioned is continuous tone. For some time, this was thought to be the absolute limiting case, which it is under the set of constraints mentioned earlier.

### Empirical versus Theory-Based $n$ -values

Although the Yule-Nielsen parameter  $n$  may assume any value, values other than 1, 2, and  $\infty$  (values of  $u$  other than 1,  $\frac{1}{2}$ , and 0) may be regarded as empirical tweaks. Ruckdeschel and Hauser did apply theory to arrive at  $n \in [1,2]$ , but it can be demonstrated that, as long as the reflectance of the solid is wavelength dependent, their methodology shall compute different  $n$  will for different wavelengths. Based on empirical observation, Iino and Berns suggested wavelength-dependent  $n$ , [12] but the Ruckdeschel and Hauser methodology was not able to predict the dependency they arrived at empirically. This is evidence of a problem with the theory. In light of both this and the rather aggressive assumptions made in its derivation, it was decided to examine some of these assumptions and the effects of relaxing them.

### Three Models of Halftone Spectra

The assumptions needed for the Yule-Nielsen model are rather aggressive. In the three models which follow, some of the assumptions shall be relaxed. All three models admit scatter within the ink layer, which shall be modeled using Kubelka-Munk [13] and a simplification of it by Tollenaar and Ernst. [14] The second assumption to be relaxed (in two of the

three cases) is that of hard-edged or sharp halftone dots in the final print. We shall model ink spread, a smearing of the ink at or after its transfer to the substrate, as a volume-preserving transformation. (This is distinct from dot gain, which in which ink volume is not preserved; it is usually increased.) Different degrees of ink spread are illustrated in Figure 1.

The models which follow continue to assume that the ink does not penetrate any portion of the substrate which exhibits significant scatter of light. Further, the second and third assume that the mean diffusion distance of light within the substrate is significantly larger than the pitch of the halftone pattern.

#### VHM-5: Complete Ink Spread, Non-Transparent Ink

In this case we consider complete ink spread. The models of Kubelka and Munk or Tollenaar and Ernst may be used to account for ink scatter. We shall first consider the latter. The Tollenaar-Ernst model was derived for the optical density of a continuous ink layer of thickness  $Z$ :

$$D_\lambda = D_{g\lambda} + (D_{\infty\lambda} - D_{g\lambda}) \left(1 - e^{-m_\lambda \cdot Z}\right) \quad (6)$$

Under Tollenaar-Ernst, what may be termed the *parametric thickness* of the solid may be written:

$$Z_s \cdot m_\lambda = \ln(D_{\infty\lambda} - D_{g\lambda}) - \ln(D_{\infty\lambda} - D_{s\lambda}) \quad (7)$$

The parametric thickness of the "tint" after ink spreading will be  $f$  times the parametric thickness of the solid, and may be substituted into the Tollenaar-Ernst forward model to obtain the density of the tint:

$$D_{t\lambda} = D_{\infty\lambda} - (D_{\infty\lambda} - D_{g\lambda})^{1-f} (D_{\infty\lambda} - D_{s\lambda})^f \quad (8)$$

This model is the single-ink VHM-5 with the Tollenaar-Ernst simplification. We may also write the single ink VHM-5 under Kubelka-Munk:

$$\beta_{t\lambda} = \frac{1 - \beta_{g\lambda} [a_\lambda - b_\lambda \cdot \coth(f \cdot b_\lambda \cdot S_\lambda \cdot Z_s)]}{a_\lambda - \beta_{g\lambda} + b_\lambda \cdot \coth(f \cdot b_\lambda \cdot S_\lambda \cdot Z_s)} \quad (9)$$

where the Kubelka-Munk parametric thickness of the solid is  $b_\lambda \cdot S_\lambda \cdot Z_s$ , and may be determined from the spectra of the solid and substrate and the  $a$  and  $b$  spectra:<sup>1</sup>

$$b_\lambda \cdot S_\lambda \cdot Z_s = \tanh^{-1} \frac{a_\lambda - \beta_{s\lambda}}{b_\lambda} - \tanh^{-1} \frac{a_\lambda - \beta_{g\lambda}}{b_\lambda} \quad (10)$$

#### VHM-6: Non-Transparent Ink, No Ink Spread

Consider once again hard-edged dots (as appear in the top of Figure 1), the same type which are assumed by Yule and Nielsen. In this section, the effect of optical scatter in the ink layer shall be accounted for. A refined version of the Clapper-Yule model [15] is offered here. (Clapper and Yule's motivation for internal reflection was the discontinuity in refractive index at the top of the print; their work assumes transparent inks.) An initial fraction  $f \cdot \beta_{0\lambda}$  of the incident flux will be reflected immediately because of the opacity of the

<sup>1</sup>Corrected version of Kubelka's Eq (25)

ink;  $\beta_{g\lambda}[1 - f \cdot (1 - T_\lambda)]^2$  will exit the substrate after one pass through the dot;  $\beta_{g\lambda}^2 \cdot \beta_{0\lambda} \cdot f \cdot [1 - f \cdot (1 - T_\lambda)]^2$  will exit after two passes through the dot, and so on, in an infinite geometric series. The ratio between two successive terms in this geometric series is  $f \cdot \beta_{g\lambda} \cdot \beta_{0\lambda}$ , and, after adding the initial reflection which is not part of this series, we obtain:

$$\beta_{t\lambda} = f \cdot \beta_{0\lambda} + \frac{\beta_{g\lambda}[1 - f \cdot (1 - T_\lambda)]^2}{1 - f \cdot \beta_{g\lambda} \cdot \beta_{0\lambda}} \quad (11)$$

which is the single-ink version of the VHM-6. Worthy of mention is that for unprinted paper, i.e., when  $f = 0$ , Eq (11) reduces to  $\beta_{t\lambda} = \beta_{g\lambda}$ , while for the solid ink, i.e.,  $f = 1$ , Eq (11) becomes:

$$\beta_{t\lambda(f=1)} = \beta_{0\lambda} + \frac{\beta_{g\lambda}T_\lambda^2}{1 - \beta_{g\lambda} \cdot \beta_{0\lambda}} \quad (12)$$

which is identical to Kubelka's Eq (37). [13] It is asserted that this model is rigorous under the Kubelka-Munk assumptions.

If the saturation reflectance spectrum of the ink,  $\beta_{\infty\lambda}$ , is known, together with the spectra of the substrate and the solid ink, the spectra  $T_\lambda$  and  $\beta_{0\lambda}$  may be computed through inversion of Eq (12) and Kubelka's Eq (32).

Eq (11) is a generalization of the VHM-1 for complete diffusion: For transparent inks,  $\beta_{0\lambda} = 0$ , while  $T_\lambda = (\beta_{s\lambda}/\beta_{g\lambda})^{1/2}$ . Substituting these into Eq (11) yields:

$$\beta_{t\lambda,transparent} = \beta_{g\lambda} \left\{ 1 - f \cdot \left[ 1 - (\beta_{s\lambda}/\beta_{g\lambda})^{1/2} \right] \right\}^2 \quad (13)$$

which, after a little algebra, yields Eq (2) with  $n = 2$ .

### VHM-7: Incomplete Ink Spread, Scattering Ink

The previous cases considered have all addressed extremes of either ink spread or ink transparency or both. More realistic is the case of incomplete ink spread, and an optically scattering ink. This case will be addressed in this section.

We continue to assume no penetration of ink into the substrate, and complete diffusion of light within the substrate. While some have admirably employed continuously variable ink layer thickness, [16, for example] we employ the "Core-Fringe" method of Azuma, et al. [17] This model of ink spread is illustrated in the bottom subfigure of Figure 1. The fractional coverage  $f$  is replaced with two fractional coverages,  $f_c$  and  $f_f$ , for core (higher density) and fringe (lower density) regions, respectively.

We impose the somewhat arbitrary constraint that the thickness of the ink layer in the fringe is half that in the core which in turn is identical to that of the solid. The volume preservation constraint then implies that  $f_c + \frac{1}{2}f_f = f$ . If the Kubelka-Munk spectra of the ink are known, the spectra  $\beta_{0f\lambda}$  (reflectance of fringe over perfect black backing) and  $T_{f\lambda}$  (transmittance of fringe) may be computed. An infinite geometric series, similar to the one in the previous section, is constructed. After adding the initial reflections caused by ink opacity it resolves to:

$$\begin{aligned} \beta_{t\lambda} &= f_f \cdot \beta_{0f\lambda} + f_c \cdot \beta_{0c\lambda} \\ &+ \frac{\beta_{g\lambda} \left[ 1 - f_f \cdot (1 - T_{f\lambda}) - f_c \cdot (1 - T_{c\lambda}) \right]^2}{1 - \beta_{g\lambda} (f_f \cdot \beta_{0f\lambda} + f_c \cdot \beta_{0c\lambda})} \end{aligned} \quad (14)$$

This model is the VHM-7 for a single ink. Because in this paper we have set the layer thickness of the core to that of the solid, we set  $\beta_{0c\lambda} = \beta_{0\lambda}$  and  $T_{c\lambda} = T_\lambda$ . When  $f_c = f_f = 0$ , Eq (14) reduces to  $\beta_{t\lambda} = \beta_{g\lambda}$ , which is expected when there is no ink. Further, when  $f_f = 1$ ,  $f_c = 0$ , Eq (14) reduces to:

$$\beta_{t\lambda(f_f=1)} = \beta_{0f\lambda} + \frac{\beta_{g\lambda}T_{f\lambda}^2}{1 - \beta_{g\lambda} \cdot \beta_{0f\lambda}}$$

which is a Kubelka-Munk expression for the reflectance spectrum of the fringe. Finally, when  $f_f = 0$ ,  $f_c = 1$ , we have analogously:

$$\beta_{t\lambda(f_c=1)} = \beta_{0c\lambda} + \frac{\beta_{g\lambda}T_{c\lambda}^2}{1 - \beta_{g\lambda} \cdot \beta_{0c\lambda}}$$

which is a Kubelka-Munk formula for the reflectance spectrum of the dot core. It is asserted that this model is also consistent with the Kubelka-Munk assumptions.

Clearly, the VHM-7 is a generalization of the VHM-6, for if we substitute  $f_f = 0$  and  $f_c = f$  into Eq (14), it reduces to Eq (11).

### Investigation of Causes of Negative n

We now turn to the question of whether either of these effects, ink spread or non-transparency of the ink, can result in a negative  $n$  to be fit by an empirical optimizer.

We have already seen that, for transparent inks, the limit of  $n$  is infinity; negative  $n$  cannot be produced by transparent inks which lie completely atop the substrate, and only when the ink spread completely. A first approach to this question is whether non-transparent inks which exhibit complete spread can cause an empirical optimizer to arrive at negative  $n$ . Halftone spectra which satisfy this may be simulated using the VHM-5.

The  $D_{\infty\lambda}$  spectrum of a set of typical process inks were computed from their Kubelka-Munk K and S spectra, as were solid ink spectra  $\beta_{s\lambda}$ . (The solid ink spectra were computed using ink layer thicknesses of 1 to 1.2 micrometers, which are typical of those used in lithographic printing.) These were substituted into Eq (8) to compute the spectra of individual ink tints for  $f = 0.1, 0.2, \dots, 0.9$ . An empirical fit of  $n$  was then performed. All fitted  $n$  were negative; those for Cyan were smallest (ranging from -4.19 to -3.36); those for Magenta were intermediate (-2.89 to -1.89); while those for Yellow were largest (-0.66 to -0.29). This is consistent with the Cyan ink being the closest to transparent (highest masstone density) and Yellow least transparent (lowest masstone density), with Magenta in between.

Having established that complete spreading of an optically scattering ink layer can cause negative  $n$ , we isolate the two effects. The VHM-6 admits scattering in the ink, but no spread. The  $T_\lambda$  and  $\beta_{0\lambda}$  spectra were computed for each ink, and single-ink tonescale spectra were simulated for the same fractional coverages as before. Here, the results were quite different. Only Yellow tints exhibited negative  $n$ , and only for some of the tone scale. The fitted  $n$  for the Cyan tints were essentially equal to 2; those for the Magenta tints ranged from

Halftone Model	Linear Mixing Space
Murray-Davies	$\beta_\lambda$
Yule-Nielsen	$\beta_\lambda^n$
Pollack's Limit	$D_\lambda = -\log \beta_\lambda$
VHM-5, using Tollenaar-Ernst	$\ln(D_{\infty\lambda} - D_\lambda)$
VHM-5, using Kubelka-Munk	$\tanh^{-1} \frac{a_\lambda - \beta_\lambda}{b_\lambda}$

**Table 2: Some halftone models and their Linear Color Mixing Spaces.**

2.11 to 2.36. Thus, it is concluded that scatter in the ink alone may produce negative  $n$ , but only for intensely scattering inks.

Finally, both transparency and ink spread are considered in conjunction with complete diffusion of light within the paper, using the VHM-7 to simulate the spectra. In order to do this, the relationship between  $f$ ,  $f_c$ , and  $f_f$  needed to be stipulated. Somewhat arbitrarily, we used the relationship:

$$f_f = 1.6 \cdot f \cdot (1 - f) \quad (15)$$

Combining this with the ink volume preservation constraint  $f_c + \frac{1}{2}f_f = f$ , yields the expression for the core area fraction:

$$f_c = f - 0.8 \cdot f \cdot (1 - f) \quad (16)$$

This model was selected for a number of different reasons, including its ability to produce core, fringe, and uninked area fractions on the closed interval  $[0, 1]$  for all  $f$  on this same interval. It does tend to produce a significant fringe area fraction which is maximized at  $f = \frac{1}{2}$ ; at this point,  $f_f = 0.8$  and  $f_c = 0.1$ .

The empirically-fit values of  $n$  using this model were 3.50 to 3.53 for Cyan, 3.84 to 4.68 for Magenta, and -3.65 to -0.55 for Yellow. As before, only the most scattering ink produced the negative  $n$ .

## Linear Color Mixing Spaces

In most of the models considered in this paper, halftone behavior can be linearly modeled in some transformation of reflectance. For example, the Yule-Nielsen-Viggiano model given in Eq (2) is linear in  $\beta_\lambda^n$ , while the Pollack limit is linear in optical density. No linear color mixing space has yet been found for the VHM-6 or VHM-7. Linear color mixing spaces for the other models are listed in Table 2.

## Conclusions

In this paper, we have re-examined the key assumptions made in some popular halftone models, derived two new models in which the assumptions of ink transparency and non-spreading inks have been relaxed, introduced the concepts of parametric thickness and linear color mixing spaces, and illustrated how scattering within the ink layer and ink spread can combine to cause an empirical determination of Yule-Nielsen parameter  $n$  to assume a negative value.

## Future Work

Future work shall include extension of the VHM-5 and VHM-6 models to multi-ink, derivation of models which admit penetration of the ink into the substrate, and models for

incomplete diffusion of light within the substrate. A systematic examination of 36 combinations of these factors is underway.

## References

- [1] J A C YULE AND W J NEILSEN [SIC]. The penetration of light into paper and its effect on halftone reproduction. In *TAGA Proceedings*, p. 65 – 76. Technical Association of the Graphic Arts, 1951.
- [2] J A STEPHEN VIGGIANO. The color of halftone tints. In *TAGA Proceedings*, p. 647 – 661. Technical Association of the Graphic Arts, 1985.
- [3] J A STEPHEN VIGGIANO. Models for the prediction of color in graphic reproduction technology. MSc thesis, Rochester, NY: Rochester Institute of Technology, 1987.
- [4] ALEXANDER MURRAY. Monochrome reproduction in photoengraving. *Journal of the Franklin Institute*, **221** : 721–744, June 1936.
- [5] F R RUCKDESCHEL AND O G HAUSER. Yule-Nielsen effect in printing: A physical analysis. *Applied Optics*, **17** (21) : 3376–3383, 1978.
- [6] MILTON L PEARSON.  $n$ -value for general conditions. In *TAGA Proceedings*, p. 415–425. Technical Association of the Graphic Arts, 1980.
- [7] WILLIAM W POPE. A practical approach to  $n$ -value. In *TAGA Proceedings*, p. 142–151. Technical Association of the Graphic Arts, 1989.
- [8] FELIX POLLACK. The relationship between the densities and dot sizes of multi-colour halftone images. *Journal of Photographic Science*, **3** (4) : 308–313, 1955.
- [9] J H LAMBERT (TRANSLATED BY DAVID DILAURA). *Photometry, or, on the measure and gradation of light, colors, and shade*. Illuminating Engineering Society of North America, 2001.
- [10] A BEER. Bestimmung der Absorption des rothen Lichts in farbigen Flüssigkeiten. *Ann. Phys. Chem.*, **86** (2) : 1852.
- [11] J S ARNEY AND S YAMAGUCHI. The physics behind the Yule-Nielsen equation. In *Final Program and Proceedings: IS&T PICS Conference*, p. 381–385. IS&T: The Society for Imaging Science and Technology, 1999.
- [12] KOICHI IINO AND ROY S BERNS. Building color-management modules using linear optimization I. Desktop color system. *Journal of Imaging Science and Technology*, **42** (1) : 79–94, 1998.
- [13] PAUL KUBELKA. New contributions to the optics of intensely light-scattering materials. Part I. *Journal of the Optical Society of America*, **38** (5) : 448–458, 1948.
- [14] DAVID TOLLENAAR AND P A H ERNST. Optical density and ink layer thickness. In *Problems in High Speed Printing: Proceedings of the Sixth International Conference of Printing Research Institutes*, p. 214–234. Pergamon, 1961.
- [15] F R CLAPPER AND J A C YULE. The effect of multiple internal reflections on the densities of half-tone prints on paper. *Journal of the Optical Society of America*, **43** (7) : 600–603, 1953.
- [16] STEFAN GUSTAVSON. *Dot Gain in Colour Halftones*. PhD dissertation, Linköping, SE: Linköping Institute of Technology, 1999.
- [17] YOSHIHIKO AZUMA, HIROMI UOMOTO, SHUNSUKE TAKAHASHI, AND MASAO INUI. Prediction of color in halftone prints using core-fringe model. In *The First European Conference on Color in Graphics, Imaging, and Vision (CGIV)*, p. 594 – 597. IS&T: the Society for Imaging Science and Technology, April 2002.

# Research on New image Screening method of Avoiding Morie Strip

Guangxue Chen, De Zhang; Xi'an Research Institute of Surveying and Map; Xi'an, China

## Abstract

*In color image printing, the halftone image must be processed. This process is called image screening. Avoiding Morie strip is the one of the cores of screening technique. Nowadays, there are two ways to avoid Morie strip. One is the FM screening; the other is AM screening in which avoiding Morie strip is by changing the screening angle. This paper brings forward a new image screening method of avoiding Morie strip, FCAM screening (Frequency conversion amplitude modulation) which is different above-mentioned two methods. It also researches on the phenomena and theorems of producing and avoiding Morie strip in FCAM screening, and draws the elementary conclusions.*

## Preface

The screen dot is the basis of composing printing image and the basic cell of expressing the color image tone. It transfers the tone of image. In the duplication of color continuous original, transferring the color and tone of original to the printed matter as verily as possible is the core of success of image duplication. After long researches and practices of human being, the modern color image duplication technology which adopts screen dot to print forms. The tradition screening method was invented 100 years ago, the digital screening theory began to form. Because the image outputting must be processed by screening, the screening technique is still the core issue of electronic publishing and image duplication in computer era.

Avoiding Morie strip is always the technical kernel issue in digital screening. In order to avoid Morie strip, we can research on following two aspects: approximating the traditional screen angle by digital screening. In the four-color printing based on AM screening technique, the Morie strip is relative with the screen angle. The traditional screening angles, namely,  $0^\circ$ ,  $15^\circ$ ,  $45^\circ$  and  $75^\circ$  are the optimal angles and can avoiding the Morie strip. In the digital screening, if these angles can be realized, the influence of Morie strip to the printed matter can be also solved effectively; Adopting new screening method. In the traditional screening method, the screen dot size varies but its position and space are fixed that are the essential causes of producing Morie strip. When the dot size is fixed and its position is uniformly distributed randomly, then the problem of Morie strip can be solved. This is the FM screening technique in modern screening techniques. In the principle of FM screening technique, any angle combinations can not produce Morie strip. So it provides the possibility of super four-color high-fidelity printing

Summarizing the methods and principles of avoiding Morie strip in image screening, we can deduce following two Theorems:

Theorem 1: using AM screening technique, when the dot images with the same screen line number are overprinted, by adjusting the overprinting angles between the dot images, the four-

color overprinting can be realized and can avoid the Morie strip. The quality of the print matter can be also acceptable.

Theorem 2: the FM screening technique can make the dot of screening image show irregular arrangement. Using this technique, when the different dot images are overprinted with random angles, it can't produce Morie strip. So the super four-color high-fidelity printing can be realized.

According the theorem 1, the current AM screening technique can realize four-color printing and its process is mature and stable. Because of the limitation of screen angle, the super four-color high-fidelity printing can't be realized. According the theorem 2, the FM screening technique can avoid producing the Morie strip and is not restricted by the screen angle. But the dot enlargement is not easy to be controlled and the demand of technology condition is very high, so its practical application is very difficult. So we should find a new screening method which not only can use the simple technology of AM screening, but also can realize the super four-color high-fidelity printing. So the essence of the problem is to find a new method which can avoid the Morie strip except the theorem 1 and 2.

After the long research on the image screening technique, the authors find the third method which can avoid the Morie strip, namely, FCAM (frequency conversion amplitude modulation) screening and summarize several rules of this method. It can avoid the Morie strip to a certain extent and solves the problem of super four-color high-fidelity printing.

## Basic Thought

To different halftone images, we can adopt the AM screening technique and alter the screen line number to avoid the Morie strip within a little scale of overprint angle. This method can realize overprinting the halftone image without producing the Morie strip. It provides new technical choice for the super four-color high-fidelity printing.

The new method does not apply the random screening technique. To every halftone image, it still applies the mature AM screening algorithm. So its practical technology is not difficult. The extents of avoiding the Morie strip vary with the differences between the screen line numbers of halftone images. Within a certain extent, the larger the differences between the screening lines are, the better the effects of avoiding the Morie strip are. In practice, under the precondition of gaining satisfactory quality of duplication, the extent of screen line numbers is limited. Generally, the screen line number is between 100 lpi and 300 lpi.

Because this method is based on the AM screening and alters the screen line numbers of AM screening among different screening images, this paper calls the new method FCAM screening temporarily. It provides more choices for the halftone image process and color image printing.

## Experimental Research

Experiment 0: first we observe the Morie strips produced when two halftone images with same screen line number are overprinted in different angles. The screen line number is 175 lpi. When the screen angle is 0°, the Morie strip is very obvious. As the screen angle increases, the Morie strip dies down. When the screen angle is 45°, the Morie strip is up to the minimum. When the screen angle becomes more, the Morie strip will reverse. The curve between the Mories strips and the screen angles is as following curve O in figure 1.

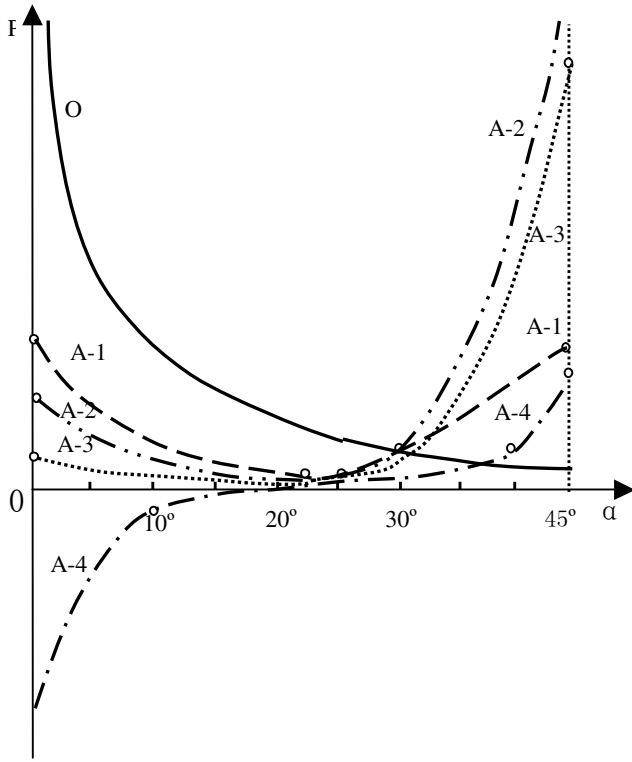


Figure 1: The trend of Morie strip

P is the space of Morie strip and  $\alpha$  is the overlap angle between the two halftone images. The curve O expresses the basic phenomena and rules of the Morie strip of the AM screening with the same screen line number.

When two screens are overlapped and one screening line number is changed, the experimental result will be as follows:

Experiment 1: we use two screens, one is 175LPI; the other is 150lpi. So the difference of screen line number is 25lpi. When the overlap angle is within 0°-45°, the strength of Morie strip is curve A-1 in figure 1.

Experiment 2: we use two screens, one is 175LPI; the other is 133lpi. So the difference of screen line number is 42lpi. When the overlap angle is within 0°-45°, the strength of Morie strip is curve A-2 in figure 1.

Experiment 3: we use two screens, one is 175LPI; the other is 120lpi. So the difference of screen line number is 55lpi. When the overlap angle is within 0°-45°, the strength of Morie strip is curve A-3 in figure 1.

Experiment 4: we use two screens, one is 175LPI; the other is 100lpi. So the difference of screen line number is 75lpi. When the

overlap angle is within 0°-45°, the strength of Morie strip is curve A-4 in figure 1.

## Analysis and Discuss of the Experimental Result

Applying FCAM screening technique, when two halftone images are overprinted, the rules of Morie strip are as following:

(1) Applying FCAM screening technique, when the overlap angle of two screens approximates to angle 0°, the Morie strip is convergent. This is different with the same screen line number screening. When two screens with the same screen line number are overlapped, from angle 0° to a certain small angle, the Morie strip is from infinite to immense. The process changes rapidly. But applying FCAM screening technique, when two screens are overlapped, the Morie strip is stable near the screen angle 0°. As the angle increases, the Morie strip changes slowly and has a fixed initial value which we call  $W_0$ . If the screening frequency and the difference of screening frequency are different, the  $W_0$  is also different.

(2) When the screening frequency of one screen is fixed, within a certain range, the larger the difference between the fixed frequency and the variable frequency is, the smaller the Morie strip is. When the difference of screen frequency is up to a certain value, the  $W_0$  is up to the minimum. Then the Morie strip is invisible, so it can be avoided.

(3) The frequency difference which makes the  $W_0$  minimum varies with the screen line numbers of two screens.

Form the experiment we can see that when the screen line number of fixed screen increases, the screening frequency difference which makes the Morie strip invisible also increases. The table 1 summarizes the relative experimental data. From it, we can see the change trend.

Table 1: The relationship between the fixed screening frequency and screening frequency difference

Fixed screening frequency (lpi)	150	175	200	225
Screening frequency difference (lpi)	50	55	67-80	75-92

From the experimental result we can draw following conclusions:

Supposing the fixed screen is  $P_1$  whose screen line number is  $n_1$ , when the screen line number of variable screen  $P_2$  decreases to  $n_2$ , namely, the difference of two screening line numbers is  $S_1(n_1 - n_2 = S_1)$ , the Morie strip is up to the minimum. When the  $n_1$  is fixed, the screen line number of variable screen  $P_2$  is up to  $n_3$ , namely, the difference of two screening line number is  $S_2(n_3 - n_1 = S_2)$ , the Morie strip is also up to the minimum.

The following equation (1) should exist:

$$\frac{S_1}{N_2} = \frac{S_2}{N_2} \quad (1)$$

(4) The CFAM screening is different with the same line number AM screening. When the Morie strip is up to the minimum, the overlap angle is not 45° but between 20° and 30°.

(5) Adopting the CFAM screening, when two screens are overlapped, the Morie strip is up to the maximum at the overlap angle 45°.

(6) When the screen frequency is up to a special value, the Morie strip can be avoided in a certain overlap angle scale or the Morie strip can be controlled in a comparatively small scale, such as the curve A-4 in the figure 1.

(7) The strength of Morie strip produced in FCAM screening is very weak. Especially, when the screen line number is up to a certain value, the strength of Morie strip is very weak at the screen angle  $0^\circ$ .

## Conclusions

The FCAM screening provides a new method to avoid the Morie strip in the halftone image screening. It is an innovation of image screening technique. According to the research in this paper, we can deduce the third theorem of avoiding Morie strip in the image screening, namely:

Apply AM screening technique, the Morie strip can be avoided in small range of overlap angle by changing the screen line number of overlapped halftone images. When the screen line number is up to special value, it can avoid the Morie strip in the same overlap angle.

Combining the theorem 1 and theorem 3, the super four color halftone images can be overlapped without producing the Morie

strip. So the super four-color high-fidelity printing can be realized based on the AM screening technique. This is one of important application fields of this research.

## Reference

- [1] Chen Guangxue, Zhang Dong, Liu Ailong, Zhang De. The Research and Application of RIP Technology in Map Publishing System. The Symposium of the 20th ICC, August, 2001.
- [2] Li Ming, Chen Guangxue, Zhang Dong. Map Publishing and RIP Technique Based on PostScript. The Bulletin of Surveying and Mapping, Vol 11, 2002.
- [3] Cheng Guangxue, Zhang Dong, The Designing Principle of the Electronic Map Publishing System Based on PostScript, The Journal of Beijing Institute of Printing, Vol 4, 1999.

## Author Biography

*Chen Guangxue(1963- ), male, doctor, researcher. Now, he works in Xi'an research institute of surveying and mapping, China. He is the committeeman of cartography and GIS committee of Chinese surveying and mapping academy. He is also the committeeman of electronic government affair of Chinese GIS committee and majors in digital cartography and GIS.*